Electronic Supplementary Material (ESI) for Environmental Science: Nano.

Supplementary Information

Laser Induced-Reduced Graphene Oxide for High Performance Electrochemical Sensors of Antipyretic Drug in Real Samples

Ravikumar Murugan[a], Kuo-Yuan Hwa[a,] *, Shih-Feng Tseng[b], Aravindan Santhan[a], and Jhih-Yi Lin[b]

[a]Department of Molecular Science and Engineering, National Taipei University of Technology, Taipei-10608, Taiwan (ROC)

[b]Department of Mechanical Engineering, National Taipei University of Technology, Taipei-106344, Taiwan (ROC)

***Corresponding author**

Kuo-Yuan Hwa, Email: kyhwa@mail.ntut.edu.tw

Tel- 02-27712171 ext. 2419 (0), 2439, 2442 (Lab)

Table of Contents

S1 Materials

$[Fe(CN)_6]^{2/3-}$ and KCl received from Sigma Aldrich, other reagents were of analytical grade. All chemical were received Sigma Aldrich and used without further purification. Different buffer solutions were made with sodium dihydrogen phosphate ($NaH_2PO_{4)}$ and disodium hydrogen phosphate ($Na_2HPO_{4)}$. Sodium hydroxide pellets and nitric acid were used to optimize the pH. All aqueous PBS solution were prepared with ultrapure water from a Milli-Q Plus system. All of the above-mentioned chemical compounds were purchased with analytical grades from Sigma Aldrich in Taiwan.

S2 Instrumentations

The functional group investigation of the all-synthesis GO and RGO was measured with Perkin-Elmer Fourier transforms infrared spectroscopy (CHI 1000 C, FT-IR-6600). The structural and the crystalline phase purity of samples were determination with XPERT PRO X-ray diffractometer (XRD) with the Cu Kα radiation. XPS- X-ray photoelectron spectroscopy (XPS) was analyzed by using a thermos-scientific ESCALAB 250. UV-Visible (JASCO V-730) was used to study bandgap of all samples. The morphological, elemental mapping, and the presence of elements were studied with the transmission electron microscopy (TEM, Tecnai G2), and energy-dispersive X-ray spectroscopy (EDAX). CV & DPV analysis as the electrochemical studies were conducted in a standard three-electrode systems (glassy carbon electrode (GCE) as working electrode, Ag/AgCl (saturated KCl) as reference electrode, and platinum wire as counter electrodes) with CHI621D electrochemical workstation (CH Instruments Company, made in the U.S.A).

S3: Real sample preparation

The real samples like human urine, river water, and pharmaceutical tablet sample were used for real sample analysis. Handling of real-samples is carried out according to institutional

review board (IRB) rules and regulations – IRB202010EM108 issued to Dr. Hwa. All the samples were pretreated separately for DPV electrochemical measurements.

S3 (A): Preparation of AP standard solution

AP was prepared using 10 mL (0.001 M) of DI water in a 10 mL volumetric flask, and shacked vigorously using a vortex for until homogenized solution. The as-prepared analyte was stored in light shield amber vial in the refrigerator at 4˚C when not in use. The AP analyte was freshly prepared before the experiment.

S3 (B): River Sample Preparation

The river water samples were collected from the Tamsui river (Taipei, Taiwan), and then samples was filtered with whatmann filter paper, and centrifuged for 15 min at 1600 rpm to get rid off dust particles. The treated river water sample 5 mL was diluted with 0.1 M PB solution (5 mL) at pH 7.0. Later, the diluted stock solution were stored in air tight plastic vials kept in refrigerator and used within a day from collection. The standard concentrations of AP (25, 50, 75, 100, and 125 μM) were spiked into the as prepared stock solution samples, transferred into 10 mL volumetric flasks, and stored at 4 ˚C. DPV technique was used to investigate the real samples analysis with RGO-3/GCE modified electrode in inert atmosphere.

S3 (C): Tablet Sample Preparation

Pharmaceutical tablet purchased from local pharmacy in taiwan, crushed to small pieces, grained as fine powder with mortar, and diluted with ethanol solvent. To remove binder, and fine particles, samples was filtered with whatman filter paper, centrifuged for 20 min at 1400 rpm to get clear AP dose solution. Further, as prepared stock solution was carried out for standard addition from 25, 50, 75, 100, and 125 μM in 0.1 M PBS to the working concentration range to electrochemical detection of AP.

S3 (D): Human Urine Sample Preparation

In brief, about 3 mL of standard biological samples, i.e., human urine is taken, homogenized with 2.0 mL of 0.1 mol L^{-1} EDTA merged with 5.0 mL of pH 7.0 Mclvaine buffer solution by using a HY-4 homogenizer model instrument, at a speed of 5000 rpm for 20 mins. As prepared stock solution samples, transferred into 10 mL volumetric flasks, and stored at 4 ˚C. Further analytical experiments are carried out using this solution in comparison to the standard addition from 25, 50, 75, 100, and 125 μM in 0.1 M PBS to the working concentration range for the electrochemical detection of AP.

Table S1: Specifications of laser patterning apparatus for laser induced RGO-1-3

IPG photonics model YLPN-1-4x200-30-M	
Specifications	**Values**
Wavelength (nm)	1064
Maximum average power (W)	30
Pulsed repetition frequency (Hz)	1 MHz
Beam diameter at $1/e^2$ (mm)	1.4 ± 0.02
Pulse width (ns)	4 to 200
Peak Power	15 kW
Spatial mode	TEM00 ($M^2 < 1.5$)
Polarization ratio	>100:1 Horizontal
Focal length of f-θ lens (mm)	105
Spot size (μm)	50 mm x 50 mm
Scanning speed (mm/s)	15
Cooling	Air Cooling (Open ATM)

Table S2: XRD and Raman data of RGO-1-3

Samples	XRD Data			Raman
	2θ values (002)	*d*-spacing	D (nm)	I_D/I_G Ratio
RGO-1	26.12	0.16	7.88	0.90
RGO-2	26.27	0.14	9.21	0.73
RGO-3	26.37	0.13	5.72	1.06

Table S3: XPS (C 1s) fitting data of RGO-1-3

Samples	C 1s Peak Binding Energy [eV]				
	C=C (sp^2)	C-C (sp^3)	C-O	C=O	COOH
RGO-1	283.6	284.4	285.9	287.8	289.8
RGO-2	283.6	284.7	286	287.7	289.8
RGO-3	283.5	284.3	286.9	287.7	289.8

Table S4: XPS (O 1s) fitting data of RGO-1-3

Samples	O 1s Peak Binding Energy [eV]		
	C-OH	C=O	C-O-C/C=O/O-H
RGO-1	534.4	533.6	531.6
RGO-2	534.8	533.2	531.5
RGO-3	536.9	534.8	532.7

Table S5: The electro active surface area values of RGO-1-3 and Randles Sevcik equation

Samples	EASA (cm^2)
Bare GCE	0.069
RGO-1	0.051
RGO-2	0.038
RGO-3	0.107
Randles Sevcik Equation	I_{pa} - Anodic peak current, n - Number of electrons
$I_{pa} = 2.69 \times 10^5 n^{3/2} AD^{1/2} C\nu^{1/2}$	A - Electroactive surface area, D- Diffusion coefficient
	C - Concentration, *v*- Scan rate

Table S6: Assessments of the Proposed RGO-3/GCE with Previous AP Sensing.

Modified Electrode	Sensitivity ($\mu AMm^{-1}cm^{-2}$	Linear range (μM)	LOD (μM)	References
SPE/CB-ERGO	0.311	9.9−95.0	0.18	[1]
f-MWCNT/GCE	0.0686	1.0−90.0	0.52	[2]
rGO−PEDOT/GCE	16.85	1−35	0.40	[3]
TC8A/AuNPs/MWCNT/GCE	7.64	1−150	0.20	[4]
AuNP-PGA/SWCNT	0.011	8.3−145.6	1.18	[5]
MWCNTs-GNS/GCE	0.0143	0.80−110	0.10	[6]
RGO-3/GCE	2.7271	0.099-1978.82	5.2 nM	This work

Table S7: Assessment of AP in spiked samples using RGO-3/GCE

Real Samples	Added (µM)	Detected (µM)	Recovery (%)
River	0	-	-
	25	24.56	98.24
	50	49.63	99.26
	75	74.68	99.57
	100	99.34	99.34
	125	124.01	99.20
Tablet	0	-	-
	25	24.71	98.84
	50	49.83	99.66
	75	74.89	99.85
	100	99.37	99.37
	125	124.41	99.52
Urine	0	-	-
	25	24.60	98.40
	50	49.64	99.28
	75	74.70	99.60
	100	99.66	99.66
	125	124.27	99.41

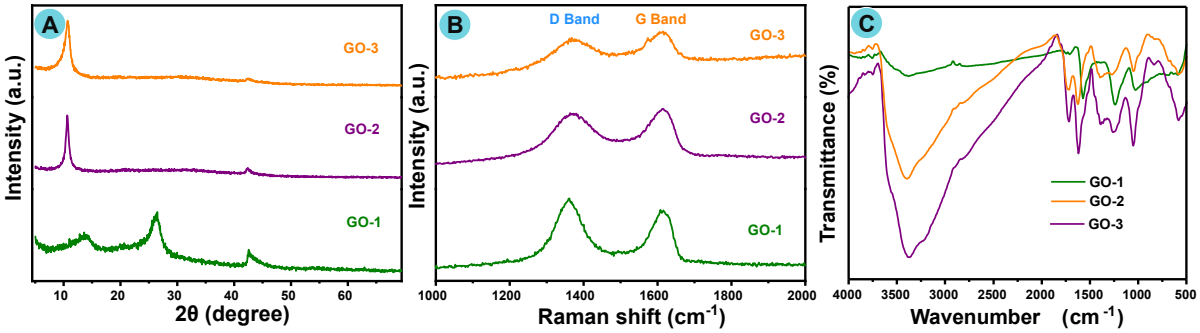

Figure S1: (A) XRD, **(B)** Raman, and **(C)** spectra of GO-1-3.

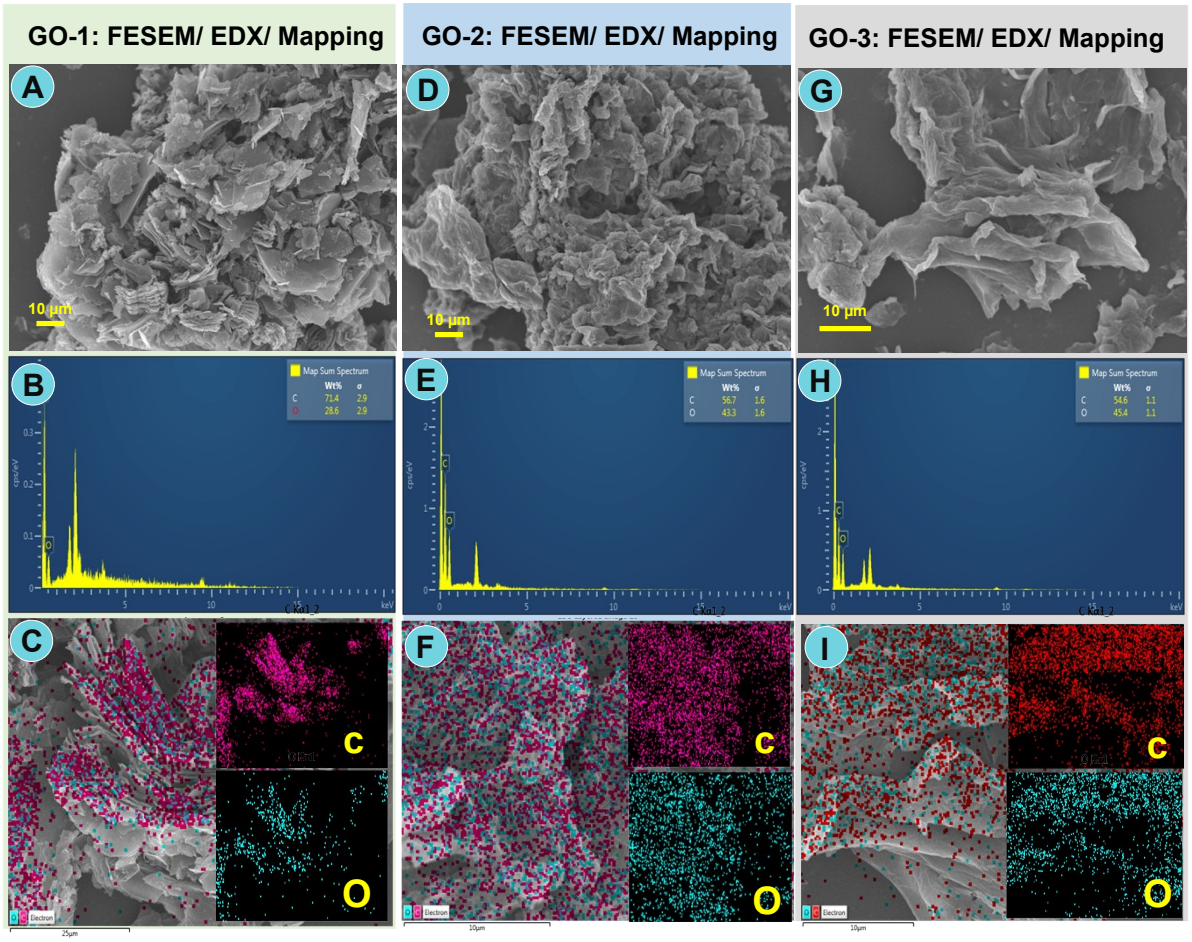

Figure S2: FESEM/EDX/Mapping of GO-1 **(A-C)**, FESEM/EDX/Mapping of GO-2 **(D-F)**, and **(C)** FESEM/EDX/Mapping of GO-3 **(G-I)**.

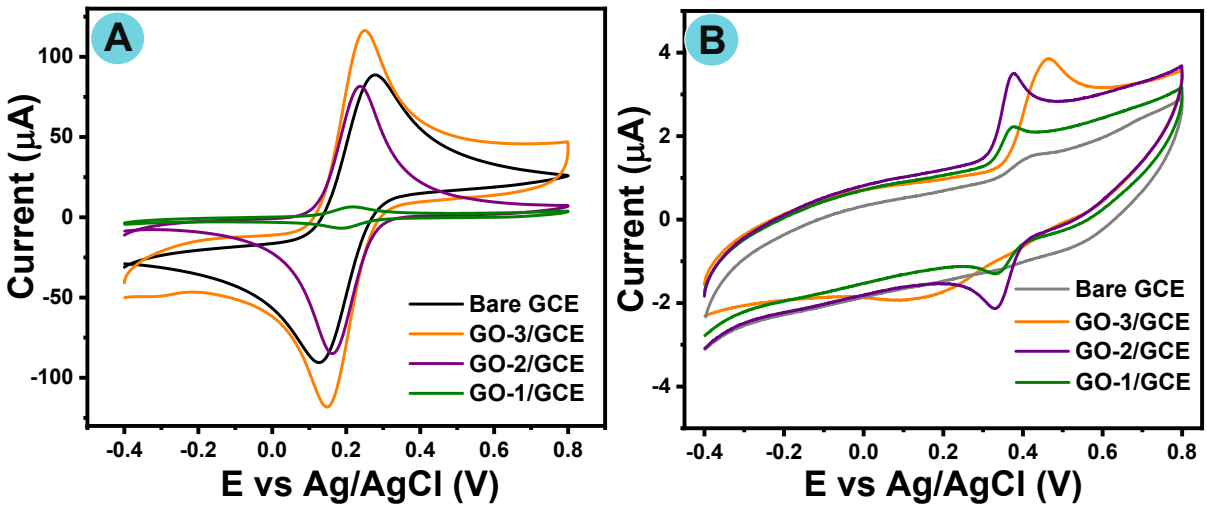

Figure S3: (A) and (B) Cyclic voltammograms response of the GO-1-3/GCE in supporting electrolyte, and PB solution with the scan rate at 50 mV/s.

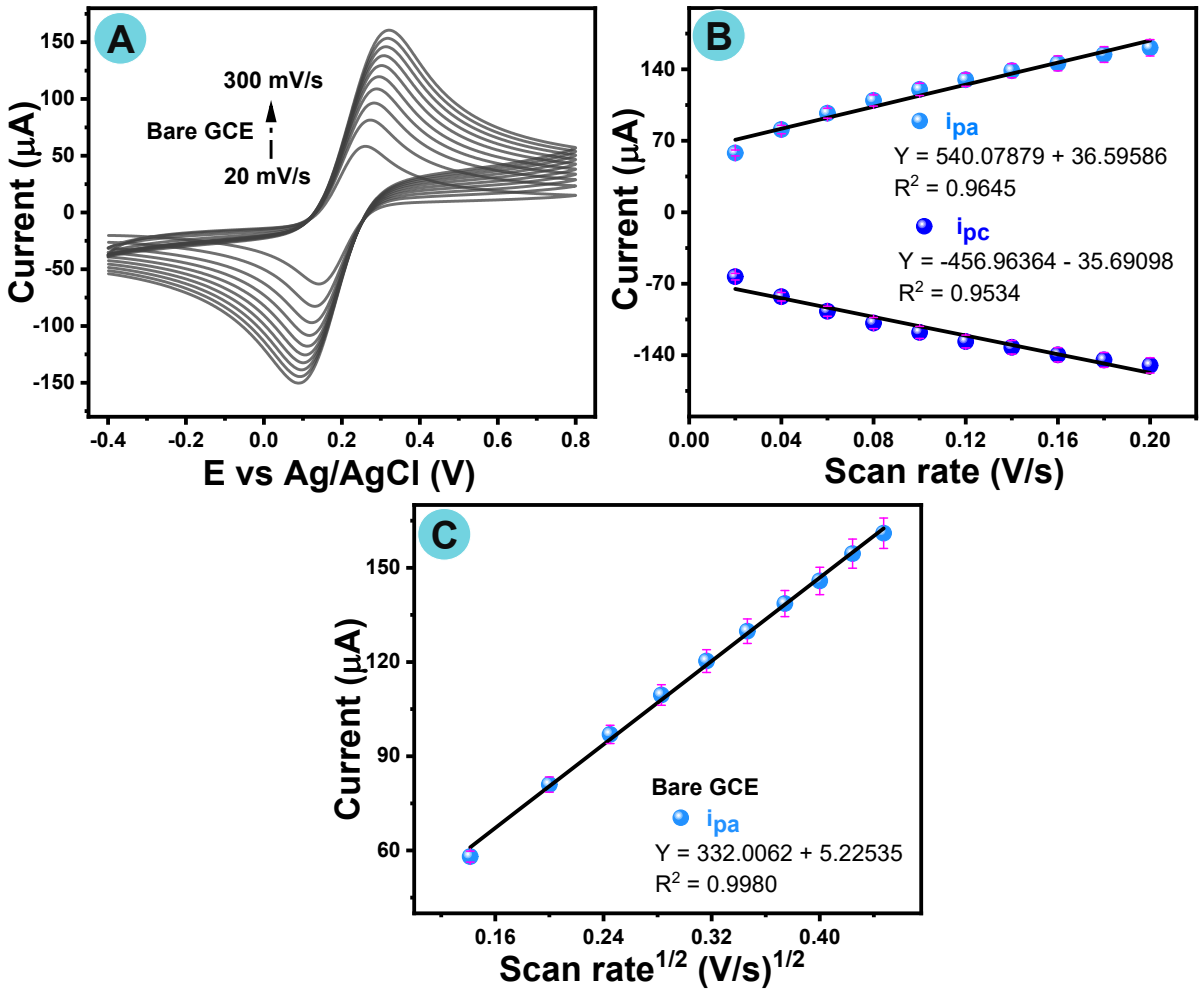

Figure S4: (A) Cyclic voltammograms of the bare GCE in 5 mM $[Fe(CN)_6]^{3-/4-}$, 0.1 M of KCl with the scan rate performed from 20 to 200 mV/s for the bare GCE; **(B)** linear plot for the scan rate (20 to 200 mV/s) vs the anodic and cathodic peak current; and **(C)** square root of scan rate vs the anodic peak current for the bare GCE.

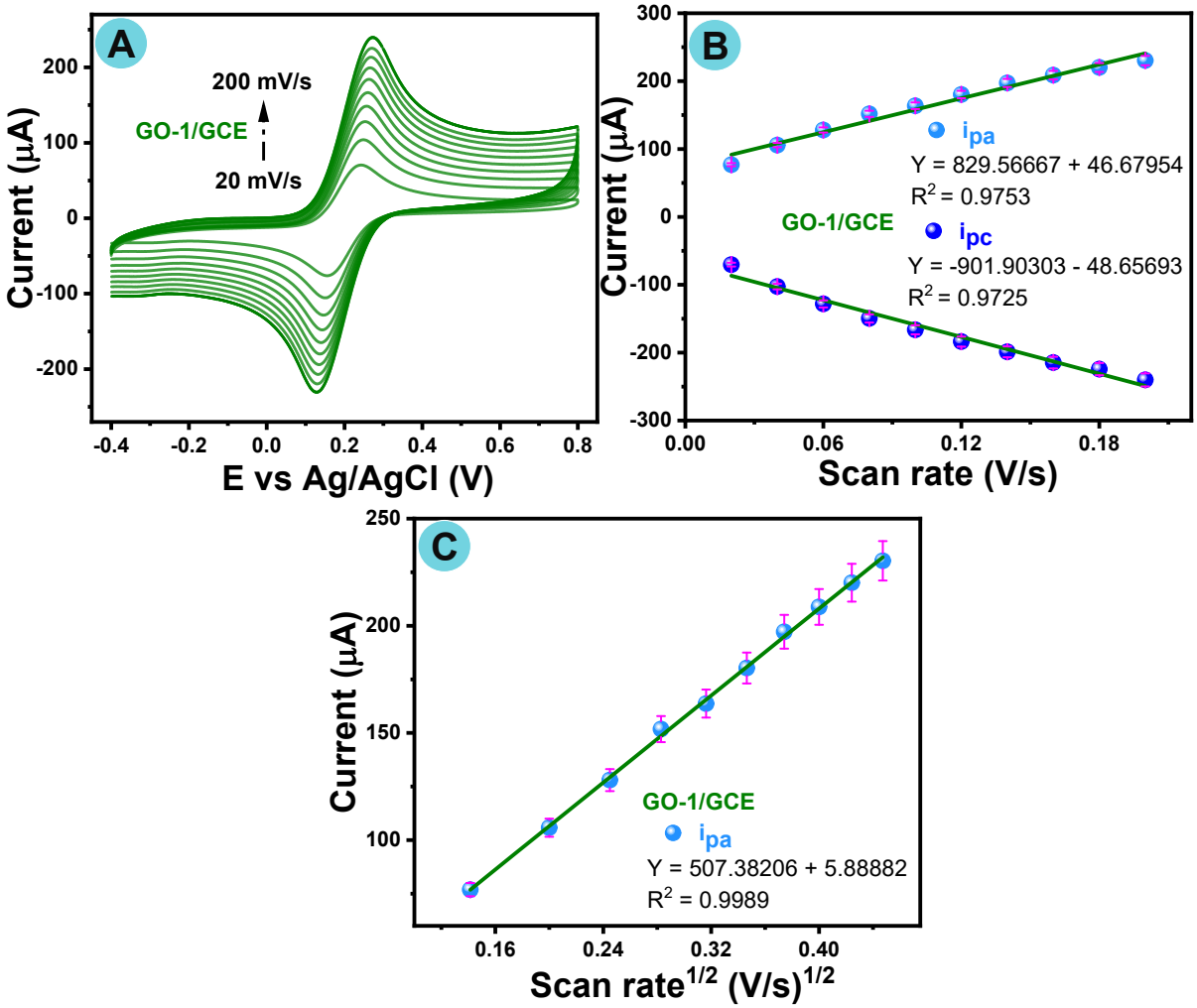

Figure S5: (A) Cyclic voltammograms of the GO-1/GCE in 5 mM $[Fe(CN)_6]^{3-/4-}$, 0.1 M of KCl with the scan rate performed from 20 to 200 mV/s for the bare GCE; **(B)** linear plot for the scan rate (20 to 200 mV/s) vs the anodic and cathodic peak current; and **(C)** square root of scan rate vs the anodic peak current for the GO-1/GCE.

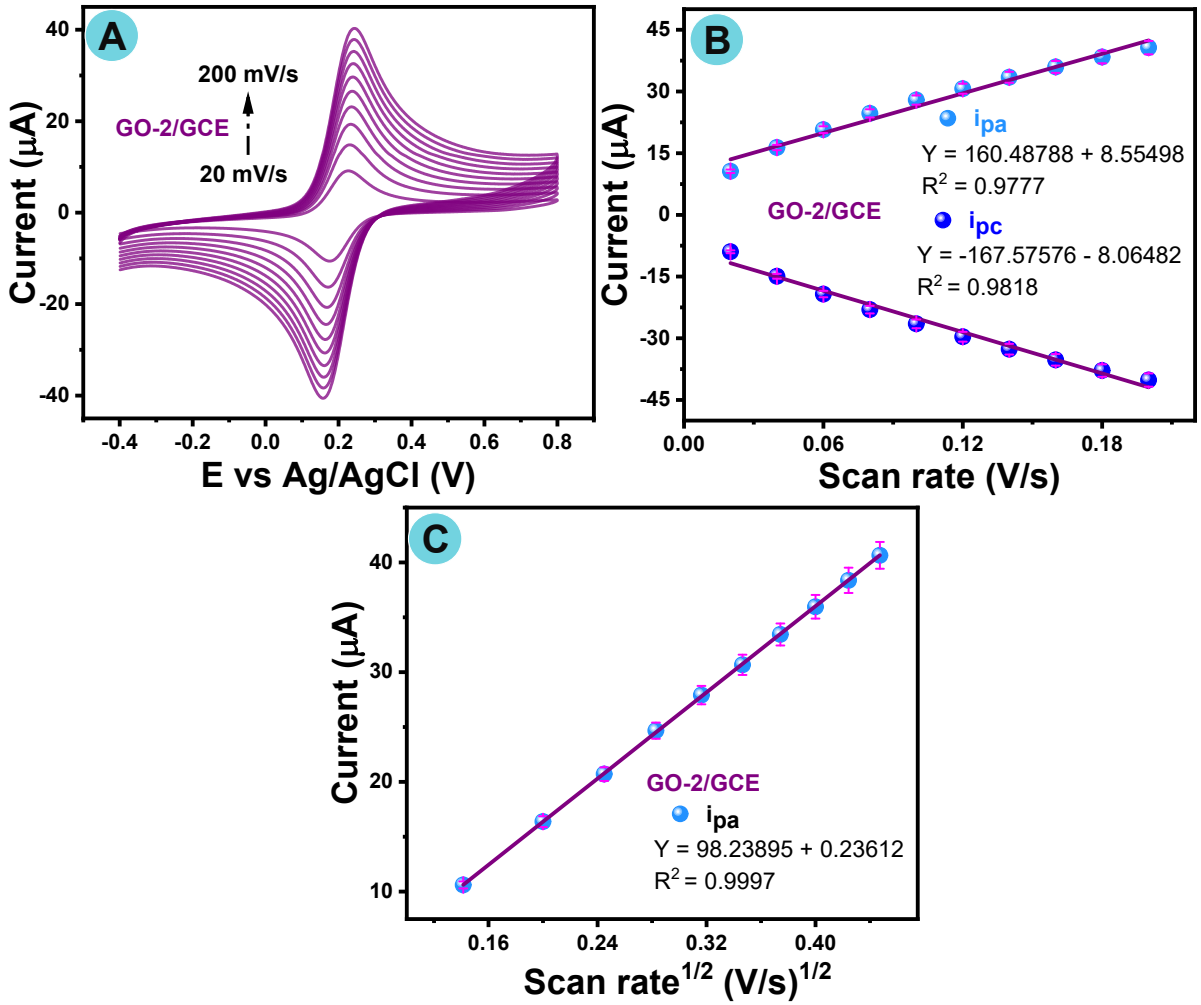

Figure S6: (A) Cyclic voltammograms of the GO-2/GCE in 5 mM $[Fe(CN)_6]^{3-/4-}$, 0.1 M of KCl with the scan rate performed from 20 to 200 mV/s for the bare GCE; **(B)** linear plot for the scan rate (20 to 200 mV/s) vs the anodic and cathodic peak current; and **(C)** square root of scan rate vs the anodic peak current for the GO-2/GCE.

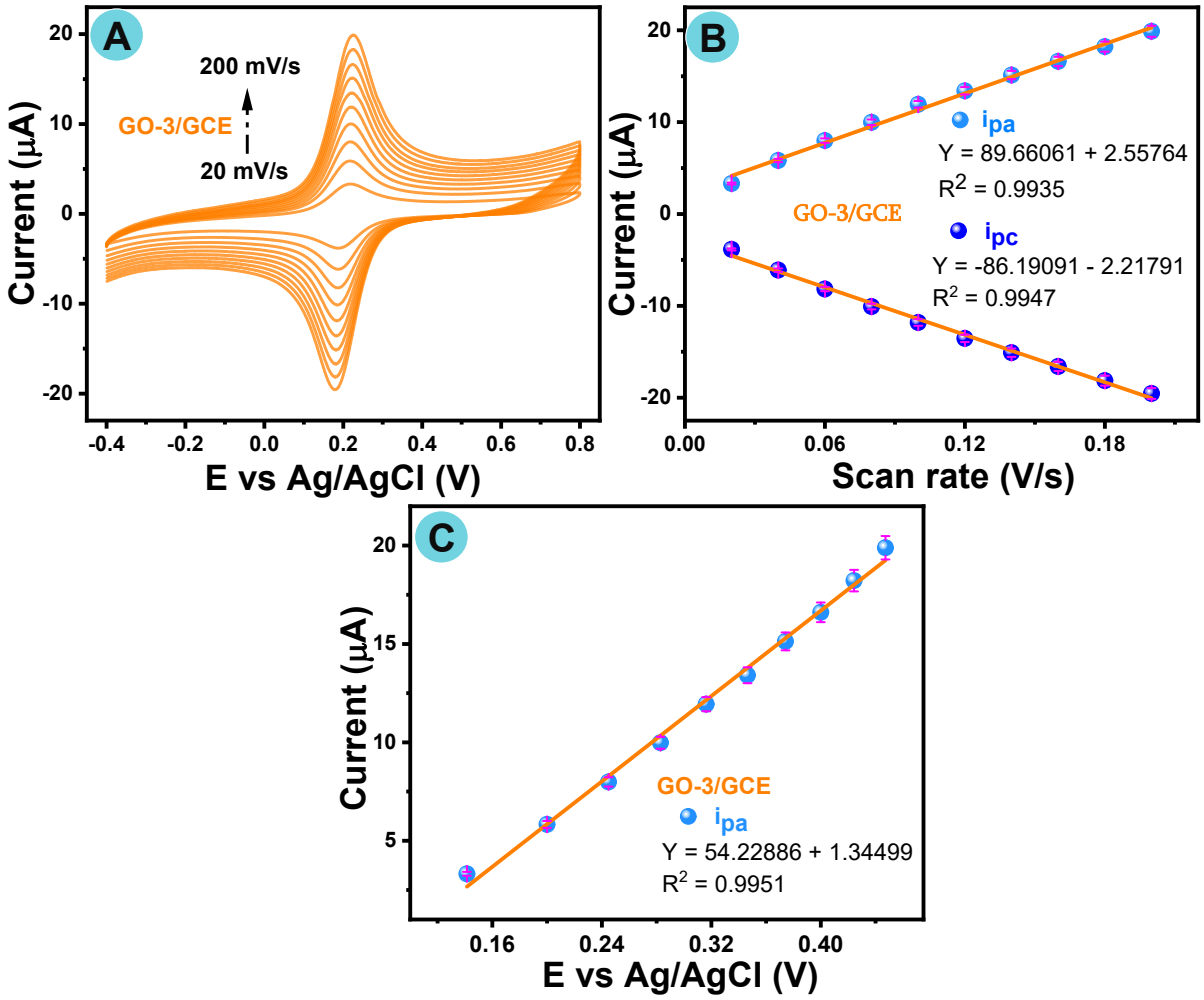

Figure S7: (A) Cyclic voltammograms of the GO-3/GCE in 5 mM $[Fe(CN)_6]^{3-/4-}$, 0.1 M of KCl with the scan rate performed from 20 to 200 mV/s for the bare GCE; **(B)** linear plot for the scan rate (20 to 200 mV/s) vs the anodic and cathodic peak current; and **(C)** square root of scan rate vs the anodic peak current for the GO-3/GCE.

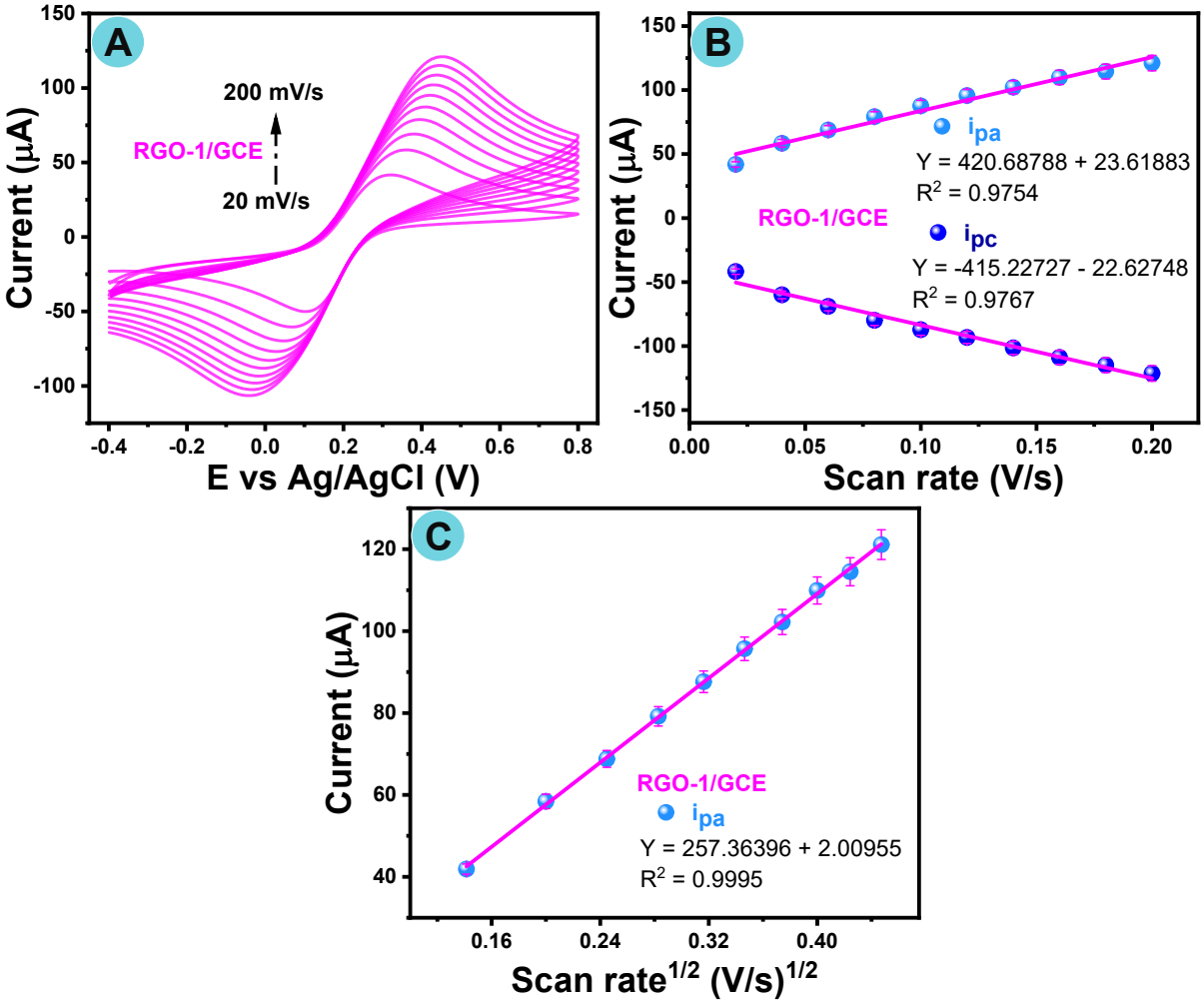

Figure S8: (A) Cyclic voltammograms of the RGO-1/GCE in 5 mM $[Fe(CN)_6]^{3-/4-}$, 0.1 M of KCl with the scan rate performed from 20 to 200 mV/s for the bare GCE; **(B)** linear plot for the scan rate (20 to 200 mV/s) vs the anodic and cathodic peak current; and **(C)** square root of scan rate vs the anodic peak current for the RGO-1/GCE.

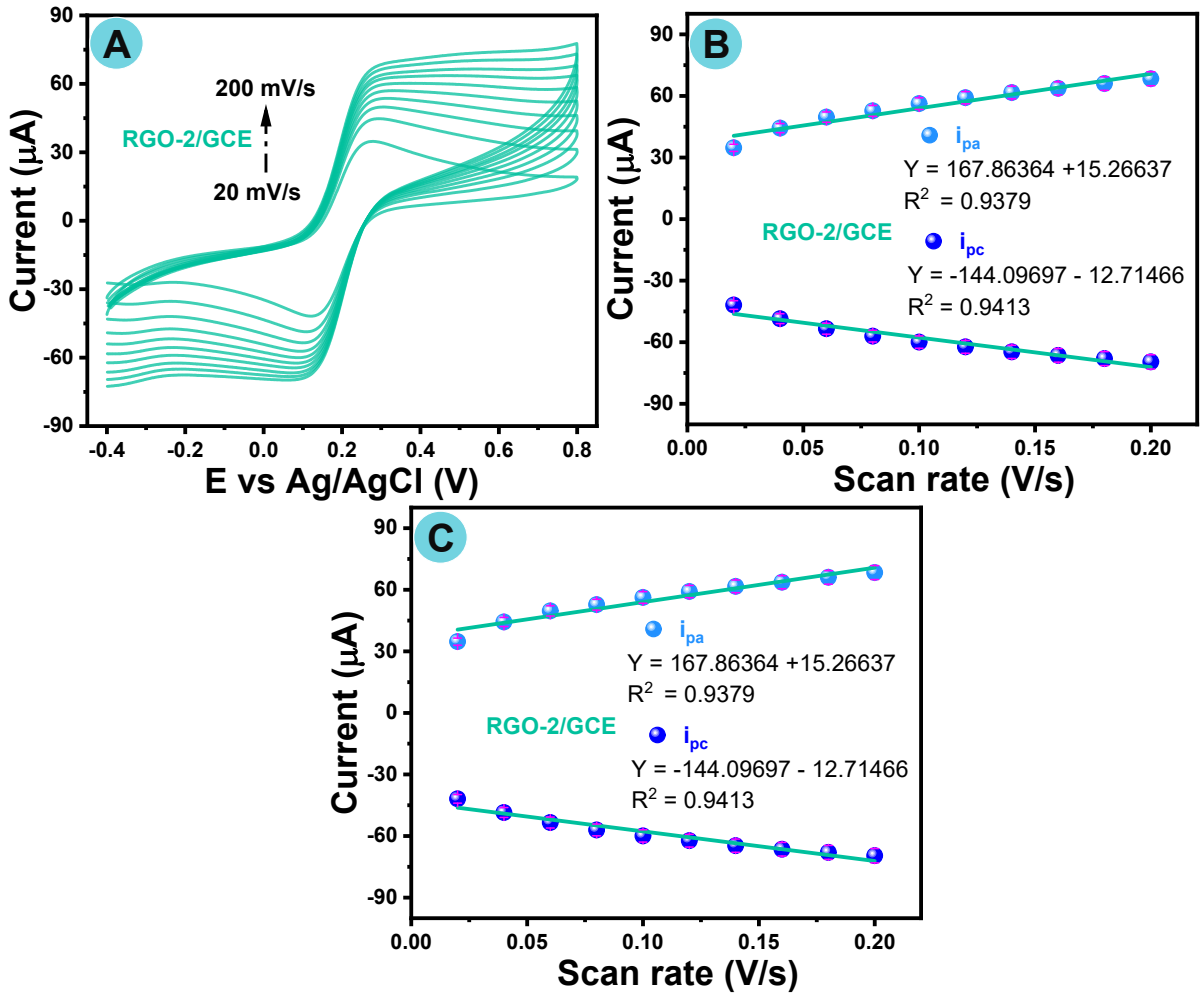

Figure S9: (A) Cyclic voltammograms of the RGO-2/GCE in 5 mM $[Fe(CN)_6]^{3-/4-}$, 0.1 M of KCl with the scan rate performed from 20 to 200 mV/s for the bare GCE; **(B)** linear plot for the scan rate (20 to 200 mV/s) vs the anodic and cathodic peak current; and **(C)** square root of scan rate vs the anodic peak current for the RGO-2/GCE.

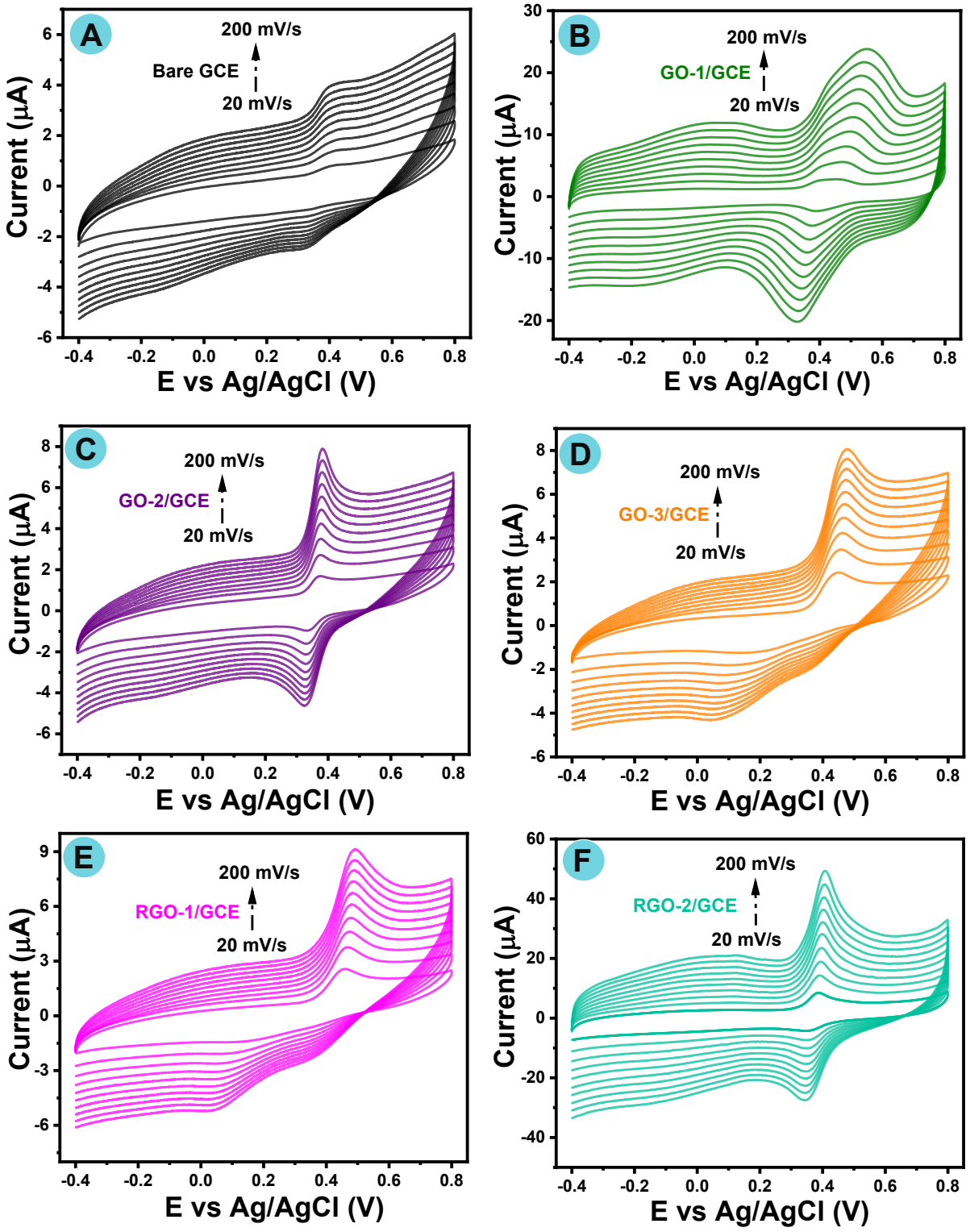

Figure S10: Cyclic voltammograms for bare GCE **(A)**, GO-1/GCE **(B),** GO-2/GCE **(C),** GO-3/GCE **(D),** RGO-1/GCE **(E),** and RGO-2/GCE **(F)** by varying the scan rate conducted from 20 to 200 mV/s in PBS solution (pH 7.0) with same concentration of AP 100 μM (0.001 M) under the inert atmosphere.

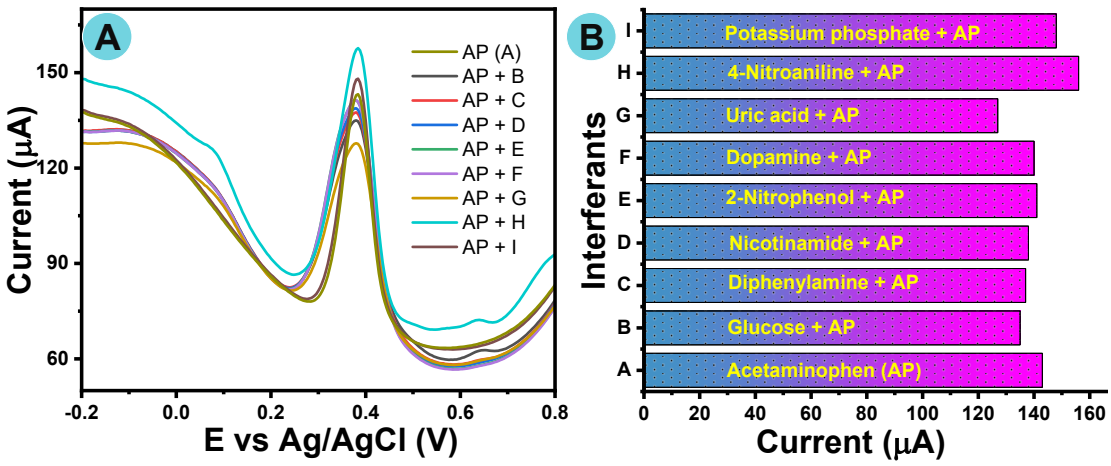

Figure S11: (A) DP voltammograms of AP with interfering compounds (1:10 folds) in PBS in N_2-purged condition with the RGO-3/GCE, and **(B)** histogram show interferants vs current.

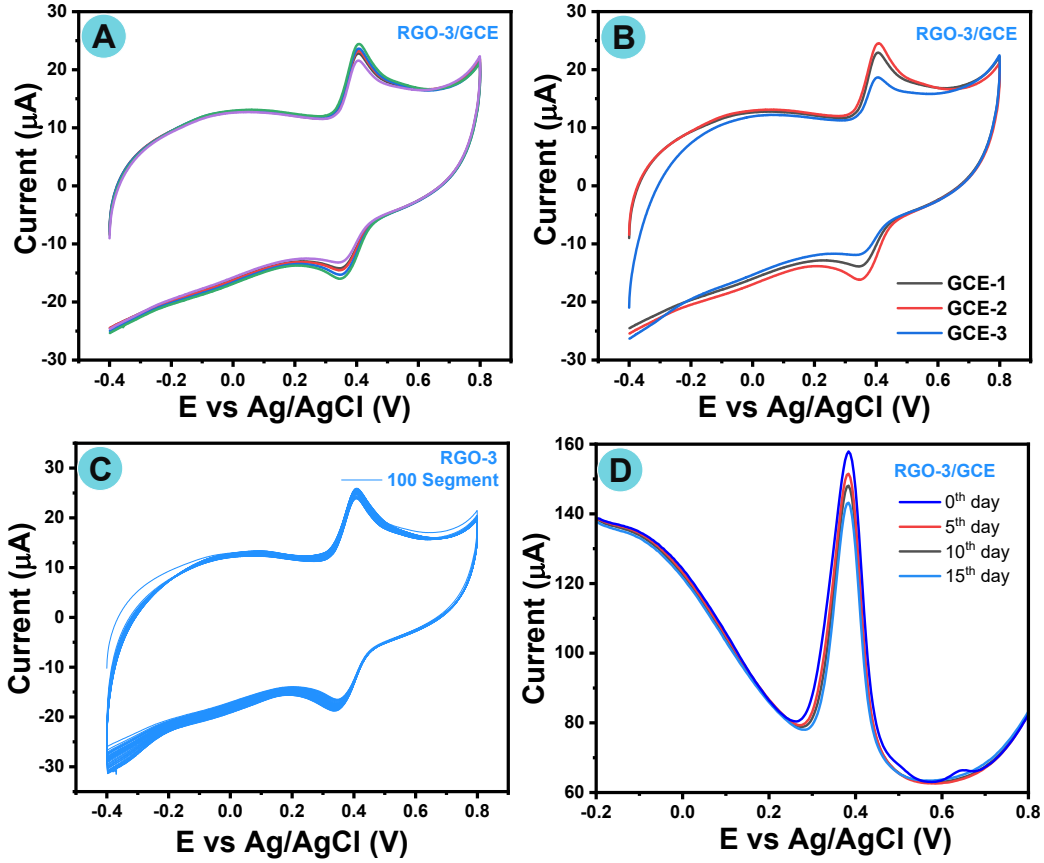

Figure S12: Cyclic voltammograms of RGO-3 modified GCE with presence of 100 µM (0.01 M) of AP in PB solution (pH 7.0) scan rate at 0.05 V/s under inert atmosphere: repeatability **(A)**, reproducibility **(B)**, cycle stability **(C),** and long-term storage stability from DPV study (**D**).

Reference:

(1) Ibáñez-Redín, G. Wilson, D. Gonçalves, D. and Oliveira, O. N., Low-Cost Screen-Printed Electrodes Based on Electrochemically Reduced Graphene Oxide-Carbon Black Nanocomposites for Dopamine, Epinephrine and Paracetamol Detection, *Journal of Colloid and Interface Science,* 2018, **515**, 101–108.

(2) Baghayeri, M. and Namadchian, M., Fabrication of a Nanostructured Luteolin Biosensor for Simultaneous Determination of Levodopa in the Presence of Acetaminophen and Tyramine: Application to the Analysis of Some Real Samples, *Electrochimica Acta* 2013, **108**, 22–31.

(3) Huang, T.-Y. Kung, C.-W.; Wei, H.-Y. Boopathi, K. M. Chu, C.-W., and Ho, K.-C. A High-Performance Electrochemical Sensor for Acetaminophen Based on a RGO–PEDOT Nanotube Composite Modified Electrode, *J. Mater. Chem. A* 2014, **2** (20), 7229–7237.

(4) Chen, Y.; Zheng, G.; Shi, Q.; Zhao, R.; Chen, M., Preparation of Thiolated Calix [8] Arene/AuNPs/MWCNTs Modified Glassy Carbon Electrode and Its Electrocatalytic Oxidation toward Paracetamol, *Sensors and Actuators B*: Chemical 2018, **277**, 289–296.

(5) Bui, M.-P. N. Li, C. A. Han, K. N.; Pham, X.-H. and Seong, G. H. Determination of Acetaminophen by Electrochemical Co-Deposition of Glutamic Acid and Gold Nanoparticles. *Sensors and Actuators B*: Chemical 2012, **174**, 318–324.

(6) Arvand, M. and Gholizadeh, T. M, Simultaneous Voltammetric Determination of Tyrosine and Paracetamol Using a Carbon Nanotube-Graphene Nanosheet Nanocomposite Modified Electrode in Human Blood Serum and Pharmaceuticals, *Colloids and Surfaces B: Biointerfaces* 2013, **103**, 84–93.